

# Cardiovascular dysfunction in adult mice following postnatal intermittent hypoxia

Alison Chu<sup>1</sup>, David Gozal<sup>1</sup>, Rene Cortese<sup>1</sup> and Yang Wang<sup>1</sup>

**BACKGROUND:** Ex-premature infants are at higher risk for hypertension and cardiovascular disease as adults, although the mechanisms underlying such increased risks are unknown. We hypothesize that postnatal exposure to intermittent hypoxia (IH) leads to cardiovascular dysfunction in adulthood with alterations of the renin–angiotensin pathway.

**METHODS:** Neonatal mice were exposed to IH for 4 wk. At the age of 3 mo, various cardiovascular measurements were obtained.

**RESULTS:** IH-exposed mice exhibited higher systolic blood pressure, impaired baroreflex responses, and decreased heart rate variability. Furthermore, IH-exposed mice manifested evidence of endothelial dysfunction, as shown by reduced reperfusion indices after tail vessel occlusion and impaired vasodilatory responses to acetylcholine. CD31<sup>+</sup> endothelial cells isolated from mesenteric arteries of IH-exposed mice expressed higher levels of angiotensin-converting enzyme and reactive oxygen species; plasma angiotensin-II levels were also significantly higher in these animals. In addition, DNA methylation patterns of the *Ace1* and the *Agt* genes in these cells were congruent with their expression patterns.

**CONCLUSION:** Our results suggest that exposures to postnatal IH alter the normal development of the renin–angiotensin system and promote the occurrence of cardiovascular dysfunction during adulthood in mice.

Recent advances in neonatal and perinatal medicine have led to increasing survival of premature infants and data on long-term outcomes of these surviving premature infants are now becoming available. Such epidemiological studies have consistently identified a strong association between prematurity and increased risk for developing cardiovascular disease during adulthood (1–6), suggesting that events occurring during early postnatal development, such as prematurity, may lead to alterations in the normal trajectory of maturation and aging of multiple organ systems, including the cardiovascular system (7–11). During gestation, interactions between the mother and the fetus are critical for optimal growth and development. Consequently, several experimental models have examined the impact of altered intrauterine environment

(e.g., maternal under- or over-nutrition) on long-term adverse consequences (e.g., cardiovascular and metabolic diseases) (12,13). In contrast, there seems to be a paucity of data on the long-term effects of postnatal environmental effects in premature infants (14).

Premature infants are at very high risk for the occurrence of frequent hypoxic events via several different mechanisms. For instance, they have immature lungs and surfactant deficiency, leading to transient hypoxia. In addition, immaturity of central and peripheral cardiorespiratory control systems may not only lead to maladaptive responses to hypoxic events but also manifest as apnea of prematurity, thereby prolonging and increasing the risk for episodic hypoxia. Many studies have shown that recurrent postnatal hypoxia affects cardiovascular regulation well into adulthood (15–19), and that calcium channels, the renin–angiotensin system, and reactive oxygen species (ROS) may underlie some of the persistent functional cardiovascular alterations, including hypertension, into adulthood (12,15,19). Given the studies that have been done, our goals for the current study are to examine the relatively unexplored role of persistent endothelial dysfunction in postnatal IH-induced hypertension in adulthood. The dynamic aspects of endothelial homeostasis, including its circulating fraction, i.e., endothelial progenitor cells and endothelial microparticles, could be altered by postnatal IH, and lead to vascular dysfunction as illustrated by both enhanced constrictive response to vasoactive agents and impaired endothelium-mediated vasodilation (20,21).

While oxidative stress is frequently involved in endothelial dysfunction in many disease conditions, it is also a common occurrence in a variety of perinatal stresses (17). In addition, animal models of cardiovascular programming in response to hypoxia have also provided evidence of increased angiotensin receptor expression and superoxide production in vascular smooth muscle cells, along with impaired endothelium-dependent vasodilation (22). Thus, the marked increase in ROS generation and propagation associated with postnatal IH could potentially lead to persistent alterations in endothelial biology and function. Based on these considerations, we hypothesized that neonatal exposure to intermittent hypoxia (IH) in a murine model would lead to the

<sup>1</sup>Department of Pediatrics, University of Chicago, Chicago, Illinois. Correspondence: Yang Wang ([ywang@peds.bsd.uchicago.edu](mailto:ywang@peds.bsd.uchicago.edu))

Received 10 March 2014; accepted 16 September 2014; advance online publication 21 January 2015. doi:10.1038/pr.2014.197

emergence of adult phenotypes of cardiovascular disease (e.g., endothelial dysfunction, hypertension, and altered baroreflex and autonomic nervous system regulation).

## RESULTS

### Body Weight

IH-exposed pups exhibited slightly smaller body weights during the exposure period at 1 (4.64 g in RA vs. 4.20 g in IH,  $P < 0.05$ ), 2 (7.65 g in RA vs. 6.89 g in IH,  $P < 0.05$ ), 3 (10.81 g in RA vs. 9.67 g in IH,  $P < 0.05$ ), and 4 (15.97 g in RA vs. 15.13 g in IH,  $P < 0.05$ ) weeks of age. However, the IH mice seemed to demonstrate faster weight accrual after the cessation of IH exposure and, at 6 wk of age and beyond, their body weights were not different from those of RA controls (Figure 1).

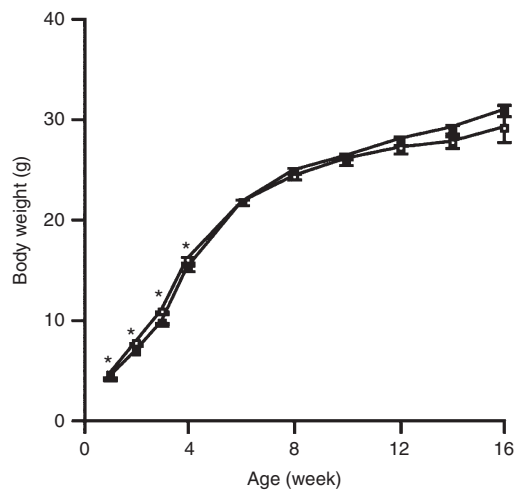


**Figure 1.** Intermittent hypoxia (IH)-exposure causes slightly decreased body weight during the exposure period only (\* indicates  $P < 0.05$ ). Shown are average body weights of the two groups of mice: room air (open boxes) and intermittent hypoxia (closed boxes). After the initial exposure period, there were no significant differences in weight, suggesting that at later weeks, IH-exposed mice demonstrated catch-up growth.

### Blood Pressure, Heart Rate Variability, and Baroreflex

Mean daily systolic blood pressures were significantly higher in IH-exposed mice ( $n = 7$ , one mouse lost telemetry signals) compared to RA controls ( $n = 8$ ) ( $114.9 \pm 2.2$  in RA vs.  $121.7 \pm 1.5$  mmHg in IH;  $P < 0.03$ ; Figure 2). However, there were no differences in either diastolic blood pressure or heart rate between the two groups.

Analysis of the baroreflex response using the sequence analysis technique (Figure 3a) demonstrated that it was significantly impaired in IH-exposed mice when compared to RA controls ( $3.2 \pm 0.2$  vs.  $2.5 \pm 0.2$  bpm/mmHg;  $P < 0.03$ ; Figure 3b). These differences were apparent both during wakefulness and during sleep (Figure 3b).

Heart rate variability, a noninvasive probe of autonomic nervous system tone, was analyzed using Poincaré plots. IH-exposed mice showed decreased heart rate variability as evidenced by reduced raw and normalized standard deviation of instantaneous beat-to-beat interval variability (SD1) and SD of continuous beat-to-beat interval variability (SD2) values during both wakefulness and sleep, suggesting higher tonic sympathetic activities in these animals (IH vs. RA for all SD values,  $P < 0.02$ ; Figure 4).

In addition, the overall decline in systolic arterial BP with the beginning of the sleep period was markedly greater in RA controls ( $-8.9 \pm 3.6$  mmHg;  $n = 7$ ) compared to IH-exposed mice ( $-1.7 \pm 3.8$  mmHg;  $n = 6$ ;  $P < 0.001$ ).

### Endothelial Function

At 12 wk of age, mice exposed to IH or to RA as neonates underwent laser Doppler flow assessments for postischemic reperfusion response, an endothelium-dependent vascular function (Figure 5a). IH-exposed mice demonstrated decreased hyperemic area (AH) and decreased hyperemia to occlusion repayment ratio (AH/AO). In addition, IH-exposed mice demonstrated shortened time to return to baseline perfusion (Figure 5b).

Endothelial function was further assessed by measuring blood pressure responses to incremental doses of acetylcholine, an endothelium-dependent vasodilator. IH-exposed

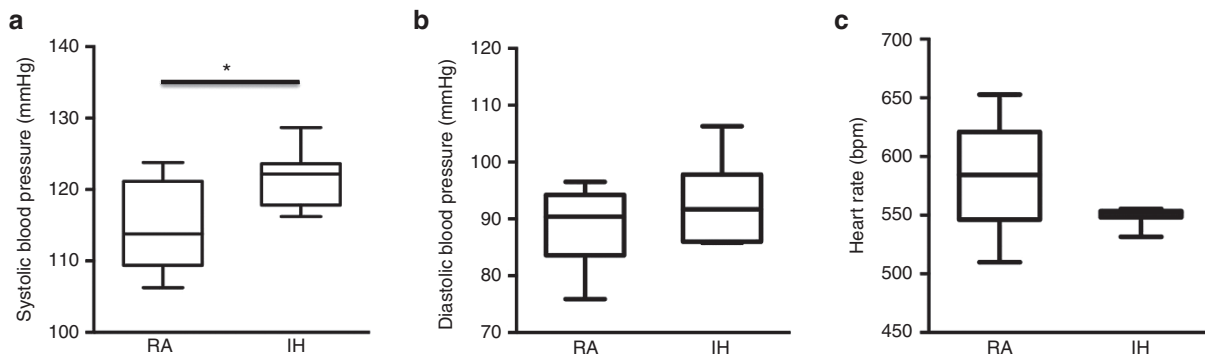


**Figure 2.** Intermittent hypoxia (IH)-exposure causes elevated blood pressure. (a) Mean circadian systolic blood pressure (RA,  $114.9 \pm 2.2$  vs. IH,  $121.7 \pm 1.5$  mmHg; \* indicates  $P < 0.03$ ;  $n = 7-8$ /group); (b) mean circadian diastolic blood pressure values (RA,  $89.1 \pm 2.5$  vs. IH,  $92.7 \pm 2.8$  mmHg;  $P = 0.36$ ,  $n = 7-8$ /group); (c) heart rate values (RA,  $583.6 \pm 16.2$  vs. IH,  $549.0 \pm 3.0$  bpm;  $P = 0.07$ ,  $n = 7-8$ /group) in the two groups of mice.

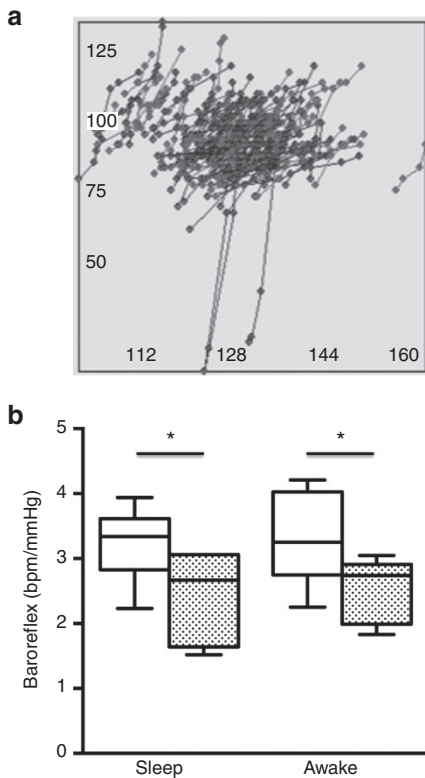


**Figure 3.** Intermittent hypoxia (IH)-exposure alters baroreflex function. (a) An example of a single analysis of the baroreflex response using the sequence analysis technique. (b) IH-exposed mice (filled boxes) demonstrate altered baroreflex function in both wake and sleep phases compared to room air mice (open boxes) (\* indicates  $P < 0.03$ ;  $n = 7-8/\text{group}$ ).

mice, when compared to RA-exposed controls, displayed diminished vasodilatory responses, especially at higher doses of acetylcholine ( $-28.8 \pm 3.1$  vs.  $-14.6 \pm 1.5$  mmHg;  $P < 0.01$ ; [Figure 6](#)).

#### Endothelial ACE Expression and ROS Content and Plasma Ang II Level

CD31<sup>+</sup> mesenteric endothelial cells were isolated from IH- or RA-exposed mice at 12 wk of age. The steady-state level of angiotensin-converting enzyme (ACE) mRNA in these endothelial cells was markedly increased in IH-exposed mice compared to RA controls ( $0.013 \pm 0.003$  vs.  $0.031 \pm 0.020$ ;  $P < 0.01$ ; [Figure 7a](#)). Furthermore, the plasma level of Ang II protein was also elevated in IH-exposed mice ( $0.101 \pm 0.009$  vs.  $0.139 \pm 0.022$ ;  $P < 0.05$ ; [Figure 7b](#)). Associated with these signs of activation of the renin-angiotensin system, mesenteric endothelial cells in IH-exposed mice exhibited increased cellular content of ROS as assessed by flow cytometry ( $105.3 \pm 10.3$  vs.  $175.4 \pm 14.5$  arbitrary units;  $P < 0.01$ ; [Figure 7c](#)).

#### DNA Methylation in Key Genes of the Renin-Angiotensin System

In line with the increased expression of ACE, the overall level of DNA methylation of a CpG island associated to the transcription start site (TSS) of the *Ace1* gene in mesenteric CD31<sup>+</sup> cells seemed to be lower in IH-exposed mice than in RA controls (RA,  $28.3 \pm 5.0$  vs. IH,  $15.9 \pm 8.1$ ;  $P = 0.214$ ; [Figure 8a](#)).

Similarly, the overall level of DNA methylation of a regulatory region containing a CTCF binding site located 3,000 bp upstream of the TSS of the angiotensinogen (*Agt*) gene also seemed to be lower in mesenteric CD31<sup>+</sup> cells isolated from IH-exposed mice (RA,  $63.1 \pm 9.8$  vs. IH,  $42.0 \pm 8.7$ ;  $P = 0.127$ ; [Figure 8b](#)).

#### DISCUSSION

In the present study, mice exposed postnatal IH demonstrated evidence of increased risk for cardiovascular disease during early adulthood, manifesting as the presence of systolic hypertension, altered baroreflex responses, and reduced heart rate variability indicative of altered balance in sympathetic-parasympathetic autonomic nervous system control. Not only does this study validate previous findings of autonomic dysregulation in a rat model of postnatal IH exposure, but it specifically supports a role for alteration in endothelial vascular function, which may act in synergy with the autonomic system to lead to increased risk for cardiovascular disease. Furthermore, increased activity of the renin-angiotensin system, as suggested by the increased expression of ACE in endothelial cells and by elevated systemic levels of Ang II, was noted in IH-exposed mice. Of note, the renin-angiotensin system has been implicated in the emergence of hypertension in adult humans subjected to IH exposures (23,24). In parallel with such findings, and possibly mechanistically associated with them, were the increased levels of ROS and decreased DNA methylation in regulatory features associated to the *Ace1* and the *Agt* genes in endothelial cells derived from IH-exposed mice. While we cannot draw definitive conclusions on the epigenetic regulation of the RAS in our animal model, as our results did not reach statistical significance, we do feel that the trend to decreased methylation in the *Ace1* and *Agt* genes does warrant reporting and further investigation. Considering that all these findings were present in the absence of somatic weight differences between IH- and RA-exposed mice, it is likely that the occurrence of IH during early life induces alterations in the programming of cardiovascular regulatory systems, affecting pathways such as the angiotensin pathways, and such reprogramming effects ultimately lead to maladaptive cardiovascular phenotypes during adulthood. This study would be one of many that reinforces the notion that exposure to adverse conditions in early life is a determinant of health and disease, and sheds light on the potential for postnatal IH as one factor in the mechanism of cardiovascular disease in ex-premature adults.

Although the effect of neonatal IH on baroreflex responses during adulthood were anticipated, those on systemic blood pressure were not. Indeed, we and subsequently others have previously shown that postnatal IH exposures promote lifelong alteration in baroreflexes and in sympathetic outflow in rats (16,19,25). The present study further expands these findings to a murine animal model, but suggests that the latter species may be less likely to compensate for the deregulation of this important homeostatic blood pressure system as evidenced by the elevation of systemic systolic blood pressures, which were absent in the rat model (19).

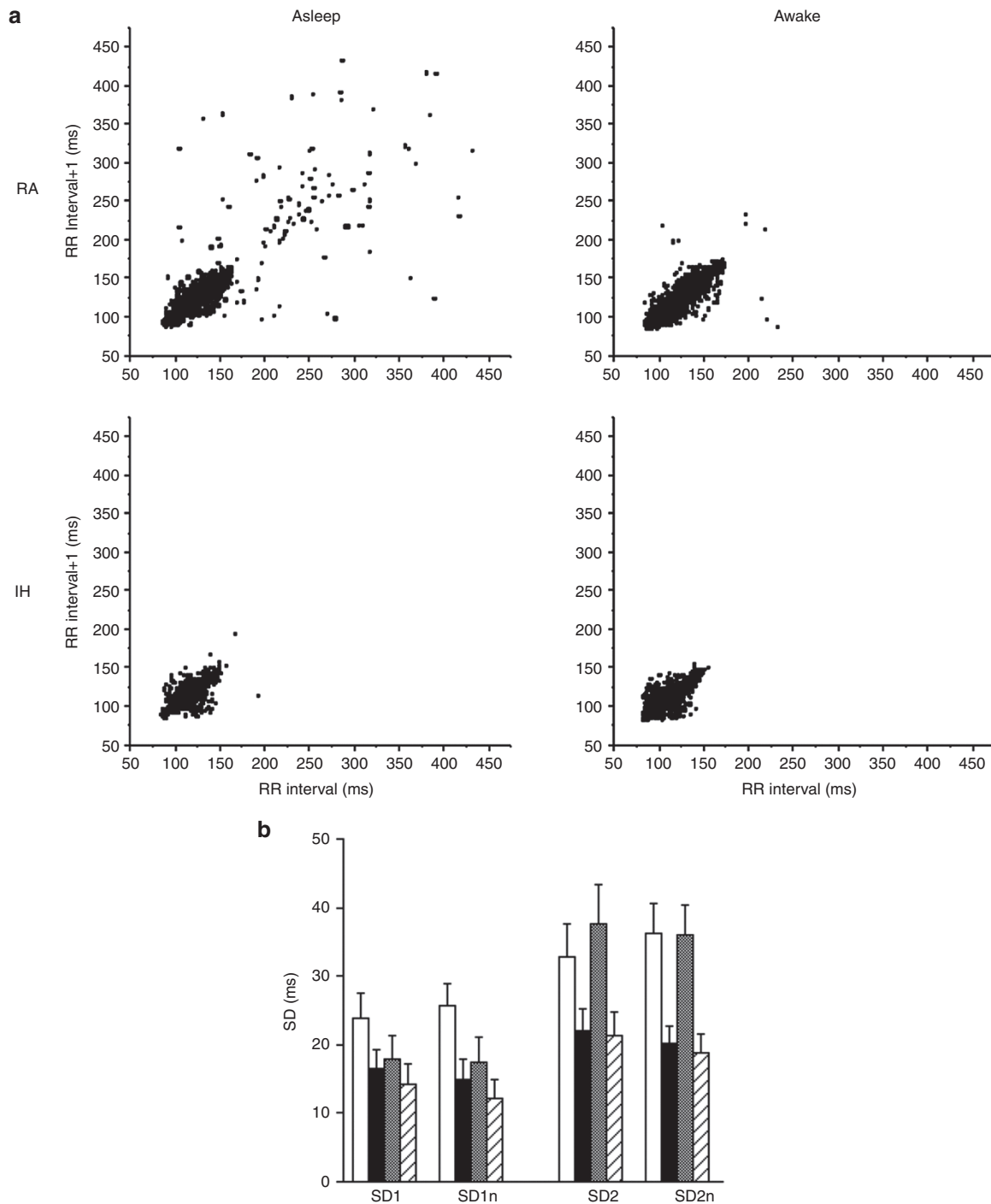


**Figure 4.** Intermittent hypoxia (IH)-exposure decreases heart rate variability (HRV). (a) Representative Poincaré plots of moment-to-moment HRV for an RA-exposed and an IH-exposed mouse during sleep and wakefulness. (b) Statistical summary of Poincaré plot indexes for RA- and IH-exposed mice during sleep and wakefulness (RA asleep, white bars; IH asleep, black bars; RA awake, gray bars; IH awake, hatched bars). IH-exposed mice showed decreased HRV, i.e., higher tonic sympathetic outflow during both rest/sleep and waking periods emerged (IH vs. RA:  $P < 0.02$ ;  $n = 7-8$ /group). *n*, normalized unit; SD1, SD of instantaneous beat-to-beat interval variability; SD2, SD of continuous beat-to-beat interval variability. All data are mean  $\pm$  SD.

These modest, but significant changes in systolic blood pressure (a difference of  $\sim 6$  mmHg) seen in our mouse model is comparable to the reported systolic blood pressure changes seen in human ex-premature infants (differences of 2.5–4 mmHg) (1,4,5). Furthermore, we now present evidence that the long-term adverse effects on baroreflex function

after IH are operational during wakefulness as well as during sleep, a state in which parasympathetic outflow is increased, as evidenced by the normal presence of BP dipping. Disappearance of BP dipping as noted in IH-exposed mice even in the absence of hypertension has adverse prognostic implications (26,27).

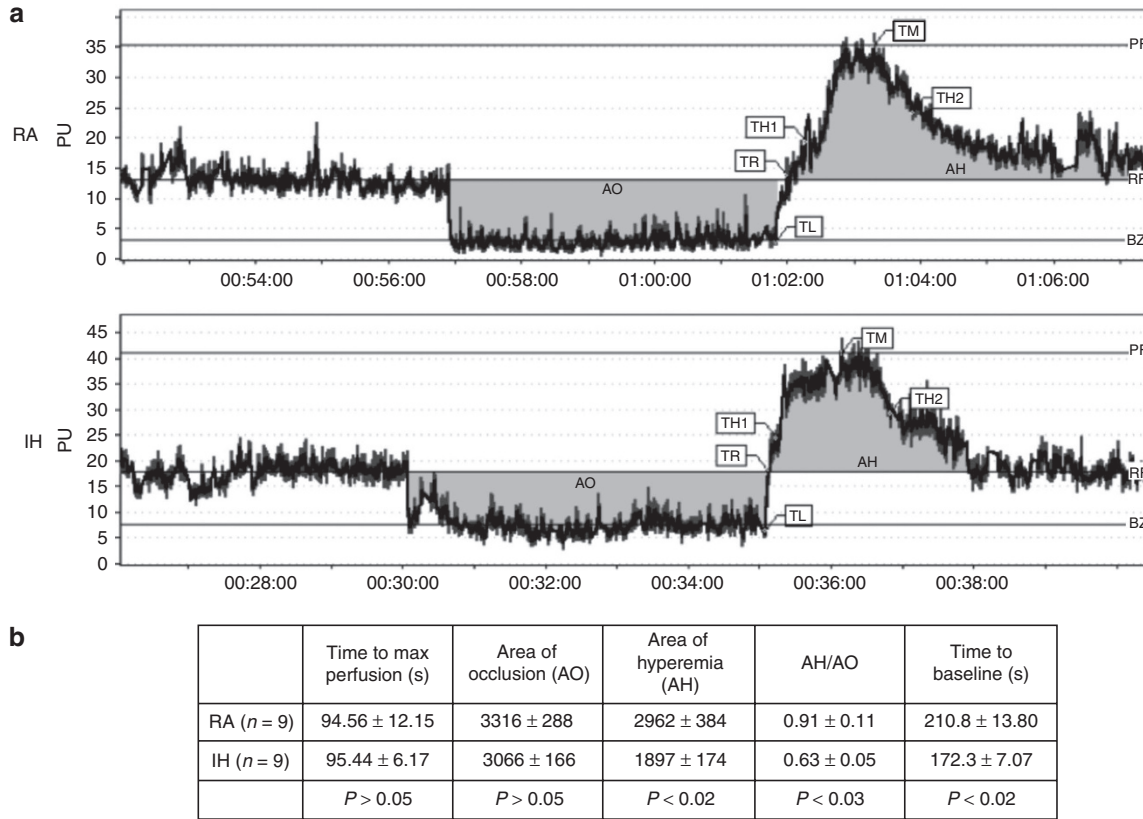


**Figure 5.** Intermittent hypoxia (IH)-exposure impairs postocclusive reperfusion function. (a) Representative laser doppler flow measurements of vascular function in for an RA-exposed and an IH-exposed mouse. X-axis is time (min) and y-axis is perfusion units (PU). (b) IH-exposed mice had impaired hyperemic reperfusion response kinetics indicative of endothelial dysfunction.

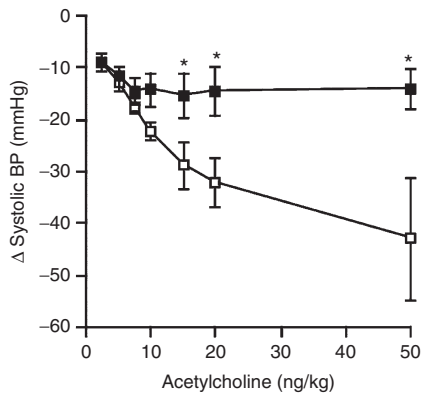


**Figure 6.** Intermittent hypoxia (IH)-exposure impairs endothelium-dependent vasodilation. Shown are blood pressure dose-responses to acetylcholine. IH-exposed mice (closed boxes) had diminished vasodilatory response at higher doses of acetylcholine (as indicated by asterisks) (RA,  $-28.8 \pm 3.1$  vs. IH,  $-14.6 \pm 1.5$  mmHg; *P* < 0.01; *n* = 3–4/group) compared to RA mice (open boxes).

Recent studies have shown a reconfiguration of carotid body function, possibly via oxidative stress-related mechanisms and epigenetic gene modifications, following recurrent apneas and IH in the postnatal period (8,28). It is unclear if and how the alterations in peripheral chemoreceptors may underlie the changes in BP regulation described herein. It should be pointed out that in addition to such localized changes in carotid bodies, these changes in BP regulation may also be

the result of substantial and extensive cellular and functional changes in central brainstem regions mediating cardiorespiratory functions (29). Taken together, current findings reinforce the notion that IH exposures, particularly if persistent or not effectively treated in premature infants may impose long-lasting modifications of the autonomic nervous system and increase the risk for cardiovascular disease later in life.

We believe that the cardiovascular dysfunction seen in this model of postnatal IH exposure results from both alteration in neural input, as evidenced by impaired HR variability and baroreflex, and disruption of local vascular, especially endothelial, function. To further explore this possibility, we examined a very early marker of ulterior adverse cardiovascular outcomes, namely endothelial cell dysfunction. Indeed, endothelial dysfunction, as demonstrated by impaired flow-mediated vasodilation, has been repeatedly found to be present in premature infants (30,31), and has been strongly associated with worse cardiovascular disease, particularly hypertension and ischemic heart disease (32,33). Here, we demonstrate the presence of diminished vasodilatory responses to acetylcholine and also reduced reperfusion kinetics as measured by laser Doppler flow studies in mice exposed to neonatal IH. We surmise that the attenuation of endothelium-dependent vasodilation is probably the result of altered nitric oxide bioavailability, which could result from increased activity of the renin-angiotensin and its downstream pathways including

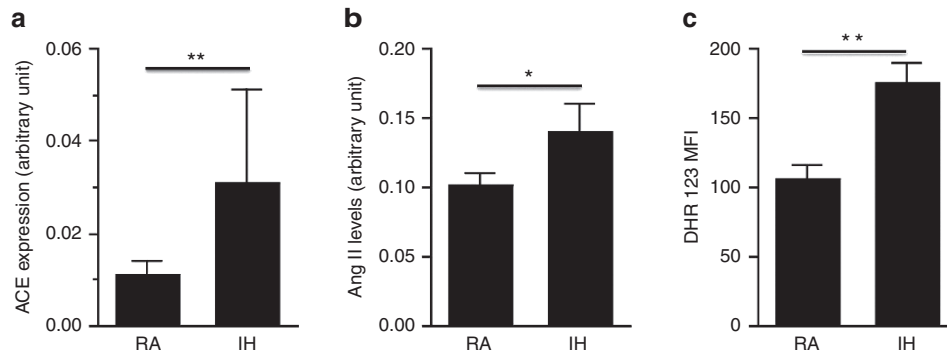


**Figure 7.** Intermittent hypoxia (IH)-exposure activates the angiotensin II pathway in CD31<sup>+</sup> endothelial cells. (a) IH increased mRNA expression levels of angiotensin-converting enzyme (ACE), assessed with real-time quantitative reverse transcription polymerase chain reaction (RA,  $0.013 \pm 0.003$  vs. IH,  $0.031 \pm 0.020$ ; \*\* indicates  $P < 0.01$ ;  $n = 8$ /group). (b) IH elevated plasma angiotensin II (ang II) levels, assessed with ELISA (RA,  $0.101 \pm 0.009$  vs. IH,  $0.139 \pm 0.022$ ; \* indicates  $P < 0.05$ ;  $n = 18$ – $22$ /group). (c) IH increased intracellular reactive oxygen species content, assessed with flow cytometry using DHR 123 as a probe (RA,  $105.3 \pm 10.3$  vs. IH,  $175.4 \pm 14.5$ ; \*\* indicates  $P < 0.01$ ;  $n = 8$ /group).

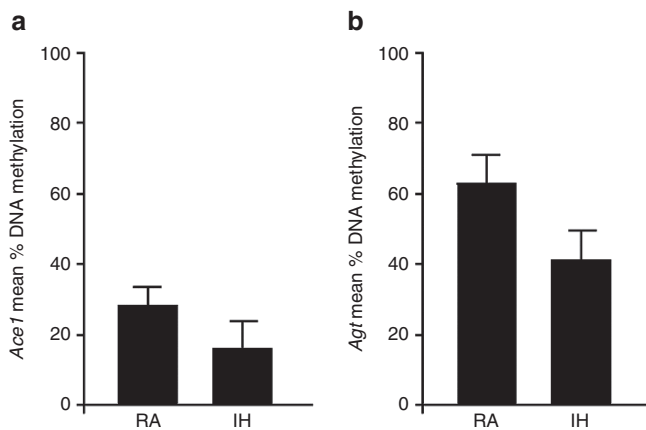


**Figure 8.** Intermittent hypoxia (IH) exposure decreased DNA methylation of key genes in the renin-angiotensin system in mesenteric endothelial cells, using DNA methylation-specific enzymatic restriction and quantitative PCR (RE-qPCR). (a) IH decreased DNA methylation of the angiotensin-converting enzyme 1 (*Ace1*) gene (RA,  $28.3 \pm 5.0$  vs. IH,  $15.9 \pm 8.1$ ;  $P = 0.214$ ;  $n = 8$ /group). (b) IH decreased DNA methylation of the angiotensinogen (*Agt*) gene (RA,  $63.1 \pm 9.8$  vs. IH,  $42.0 \pm 8.7$ ;  $P = 0.127$ ;  $n = 9$  and  $n = 11$  for RA and IH, respectively).

increased oxidative stress (34). Our findings demonstrate evidence of both increased levels of Ang II in the circulation, and increased endothelial cell expression of ACE along with elevated ROS levels in endothelial cells from mice exposed to neonatal IH. Moreover, we showed a clear trend, although not statistically significant, towards decreased DNA methylation at regulatory features associated to the *Ace1* and the *Agt* genes in these cells from IH-exposed mice compared to RA controls. Epigenetics is the collective heritable changes in phenotype due to processes that arise independent of primary DNA sequences, of which alterations in DNA methylation is one mechanisms. Our findings support the idea of an epigenetic dysregulation of these genes by neonatal IH, although the results were limited by the amount of cells available for the study. More robust studies using a larger number of animals and cells will be required to conclusively demonstrate this hypothesis. Although the source of persistently elevated ROS was not delineated in the current study, it is nevertheless

remarkable that such changes in Ang II, ACE, and ROS are still detectable 3 mo after cessation of IH, and could possibly persist for many months thereafter. These findings likely implicate activation of epigenetic mechanisms in various selected genes that specifically affect the endothelium in addition to the autonomic nervous system and chemosensory cells in the carotid body. Therefore, it is not implausible that postnatal IH will effectively lead to major epigenetic modifications in gene pathways involved in endothelial cell biology and function, consequently resulting in long-lasting alterations in renin-angiotensin system regulation and endothelial function, and ultimately leading to hypertension. While the mechanisms underlying these changes are unknown, various investigators have shown evidence of epigenetic regulation of hypertension models and the RAS (35). Future studies are planned to assess these possibilities, in order to better characterize a cause-and-effect paradigm, and to explore the endothelial methylome in IH- and RA-exposed mice. There is no doubt that further efforts to identify such epigenetically-modified gene networks are warranted such that effective therapeutic strategies aiming at preventing the adverse cardiovascular outcomes of prematurity could be developed.

## METHODS

### Animals

Pregnant dams of wild-type C57BL/6J mice at E13-15 were purchased from Charles River Laboratories (Wilmington, MA). Animals were housed in cages with 12-h light/dark cycle (light on 7:00 am to 7:00 pm) in constant temperature ( $24.0 \pm 0.5$  °C) with *ad libitum* access to food and water throughout the experiment. After birth, litter sizes were culled to six pups per litter to ensure adequate and standardized nutrition until weaning (pups were chosen based on being close to the mean body weight of all pups in each litter). Twelve litters per group were used in each experimental group. All experimental protocols were approved by the Institutional Animal Use and Care Committee (University of Chicago, Chicago, IL) and are in close agreement with the US National Institutes of Health (Bethesda, MD) *Guide for the Care and Use of Laboratory Animals*. Every effort was made to minimize animal suffering and to reduce the number of animals used.

### Postnatal IH Exposures

Animals were exposed to IH as previously described (36). Briefly, pups and their lactating mothers were housed in custom-designed

environmental chambers (Oxycycler model A44XO, BioSpherix, Redfield, NY), and were exposed to alternating cycles of 8% and 21% F<sub>2</sub>O with 120-s cycle duration for 6 h per day from 7:00 am to 1:00 pm (IH) or similar alternations consisting of 21% and 21% F<sub>2</sub>O (room air control; RA) for the first 4 wk of life. Pups were kept with their mothers until weaning at 4 wk of age. Once weaned, male offspring mice were retained and were individually housed in room air until they reached 3 mo of age, at which time experiments described below were performed.

### Body Weight Registration

Body weight was assessed weekly until 4 wk of age, then every 2 wk thereafter, always at the same time of the day, i.e., 1:00 pm.

### Blood Pressure, Heart Rate Variability, and Baroreflex Assessments

At 14 wk of age, male offspring mice (eight RA and eight IH) underwent surgery for telemetry device implantation (HD-X11 transmitters; Data Sciences International; St Paul MN). After a 2-wk recovery period that allowed animals to return to presurgical body weight and normal food consumption and weight accrual, mice underwent continuous recording of ECG and blood pressure for 48 h.

At least 1 wk after these experiments, mice were anesthetized with 1.5% isoflurane and injected with incremental doses of acetylcholine (2.5–50 ng/kg) as an i.v. bolus into the inferior vena cava to assess vasodilatory responses. Between each bolus injection, heart rate and blood pressure were allowed to stabilize for 5–10 min. Mice were sacrificed after this series of experiments.

For all these experiments, arterial waveforms were analyzed using commercial software (Dataquest A.R.T, Data Sciences International, New Brighton, MN) to derive beat-to-beat systolic, diastolic, and mean blood pressure values, as well as corresponding cardiac frequency.

Baroreflex sensitivity was estimated using the sequence method, which measures the response of cardiac frequency changes in consecutive heart beats following spontaneous changes in blood pressure. This approach was selected as it is particularly suitable for providing information on dynamic baroreflex control during spontaneous behaviors, and is particularly suited to unobtrusive telemetric recordings such as those carried herein. To this effect, baroreflex sensitivity was analyzed using the HemoLab software (version 16.0) (Harold Stauss Scientific, Iowa City, IO) that was graciously provided by Dr. Harald Stauss from the University of Iowa and was expressed as baroreflex gain (beats/min/mmHg). Telemetric tracings of 1-h duration during the beginning of the awake (between 8–10 pm) and the sleep periods (between 8–10 am) were analyzed after visual inspection of the recordings and artifact removal by an investigator that was blinded to the experimental condition (IH vs. RA). The following parameters were used: (i) correlation coefficient of 0.85, (ii) blood pressure threshold of 15 mmHg, and (iii) lag of four beats, as used by Braga *et al.* (37).

Moment to moment heart rate variability analyses were performed using Poincaré plots, by plotting any R-R interval (RR(*n*)) on the x-axis and the subsequent RR interval (RR(*n*+1)) on the y-axis for the duration of the recordings (38). A quantitative analysis of the Poincaré plot was also performed on the R-R interval time series and the following parameters were calculated from each individual scatter gram, as described by Tulppo *et al.* (39): SD of the instantaneous beat-to-beat variability of the data (SD1), and standard deviation of the continuous long-term R-R intervals (SD2). SD1 and SD2 are reported in absolute values and in normalized units (SD1*n* and SD2*n*, respectively), obtained by dividing the absolute value by the average R-R interval and then by multiplying by 1,000.

### Endothelial Function Assessment

Endothelial function was assessed using a hyperemic test after cuff-induced occlusion of the mouse tail. All testing was performed after allowing a return to baseline activity levels after placement in a full body restrainer with the tail being exteriorized and gently immobilized. A laser Doppler sensor (Periflux 5000 System integrated with the PF 5050 Pressure Unit, Perimed, Järfälla, Sweden) was applied. After 5 min of baseline measurements were acquired with satisfactory perfusion signals (PFU between 10–24), the cuff pressure was raised

to suprasystolic values for 5 min, after which the cuff was deflated to assess hyperemic responses. The reproducibility of the laser Doppler flowmetry using the Periflux system has been described previously (40). Using Perimed software, values for time to peak perfusion (Tm), area of occlusion (AO), area of hyperemia (AH), AH/AO ratio, and time to baseline perfusion (TB) were calculated.

### Isolation of Endothelial Cells

Mice were sacrificed and their mesenteric arteries were dissected from the gastrointestinal tract and washed in ice-cold PBS three times. Vessels were minced and digested in a cell isolation solution containing KREBS buffer, 20 mmol/l HEPES, 1% bovine serum albumin, 5 mmol/l glucose, and 3.5 mg/ml collagenase I (Worthington Biochemical, Lakewood, NJ) at a ratio of 1 g tissue/3.5 ml. The mixture was incubated at 37 °C with shaking at 30–40 revolutions per minute for 45 min and then centrifuged at 500 × g for 5 min at 4 °C. The floating layer was transferred into a new tube, and the pellet resuspended with 3 ml isolation solution and placed on ice for 3 min. The top 2.5 ml containing the single cell suspension was then transferred into a tube on ice. The original floating layer was added back to the remaining 0.5 ml and underwent a second digestion. Single cell suspensions from the two digestions were combined and cells were washed with culture medium once and counted. The suspension was then centrifuged at 300 × g for 10 min, and the supernatant aspirated completed. The pellet was resuspended in cell separation buffer containing CD31 microbeads (Miltenyi Biotec, Auburn, CA) at the manufacturer's suggested ratio and incubated in the refrigerator for 30 min. Cells were loaded into a magnetic column and incubated for 10 min. After the removal of supernatant, CD31<sup>+</sup> cells were washed down from the column with separation buffer. After wash, the cells were centrifuged at 500 × g for 5 min at 4 °C and resuspended in culture medium. Purity of all preparations was confirmed with flow cytometry using a different CD31 antibody (Biolegend, San Diego, CA).

### Assessment of ACE mRNA Expression

Total RNA was extracted from the purified CD31<sup>+</sup> cell population using the RNeasy micro kit (Qiagen, Valencia, CA). Following reverse transcription, real-time polymerase chain reaction (PCR) with SYBR Green dye (Life Technologies, Carlsbad, CA) was performed using a primer pair crossing intron 1 of the mouse ACE 1 gene: sense: 5'-CGC ACG ACA CCA ACA TCA C-3' (exon 1); antisense: 5'-GCC AAA TGG ACT CAT ACA ACT CC-3' (exon 2). A primer pair amplifying the mouse β-actin was used as the internal control: sense: 5'-GGC TGT ATT CCC CTC CAT CG-3' (exon 2); antisense: 5'-CCA GTT GGT AAC AAT GCC ATG T-3' (exon 3). All amplicons were subjected to melting curve analysis.

### Measurements of Plasma Angiotensin II (Ang II) Levels

Plasma samples were acidified and peptides extracted using C-18 columns (Phoenix Pharmaceuticals, RK-SEPCOL-1, Burlingame, CA), after which Ang II was assayed using an Ang II enzyme immunoassay kit (Phoenix Pharmaceuticals, EK-002-12) according to the manufacturer's instructions.

### Analysis of Endothelial Cell ROS Content

CD31<sup>+</sup> cells isolated from mesenteric arteries were analyzed with flow cytometry using a second CD31 antibody (Biolegend) and a ROS probe DHR 123 (Life Technologies). CD31<sup>+</sup> populations were gated and their DHR 123 median fluorescence intensity (MFI) was calculated using FlowJo software (Tree Star, version 9.6.2, Ashland, OR).

### DNA Methylation Analysis of the *Ace1* and *Agt* Genes

DNA was isolated from CD31<sup>+</sup> mesenteric endothelial cells using phenol-chloroform extraction and ethanol precipitation. The DNA methylation content was analyzed using DNA methylation-sensitive enzymatic restriction and quantitative PCR. After purification, 50 ng of DNA were digested with 1 unit of DNA methylation-sensitive enzymes (*HpaII*, and *HinPI*, New England Biolabs, Ipswich, MA) by incubation at 37 °C for 1 h followed by heat inactivation at 65 °C for 20 min. These enzymes cut the DNA only when the CG at the restriction site is not methylated. As a control, 50 ng of DNA were incubated under the same conditions but without the restriction enzyme. Digested and control DNA samples were then used as templates for

real-time PCR with the following conditions: 3.6 ng of DNA, 1× ABI master mix containing Taq polymerase, dNTPs, SYBR green dye, and ROX as passive dye (Life Technologies) and 200 nmol/l of specific primers. Each reaction was run in duplicate. The PCR program started with a Taq polymerase activation step (10 min at 95 °C) followed by 40 cycles at 95 °C for 15 s, 60 °C for 1 min, and 95 °C for 15 s. For the *Ace1* gene, the region of interest was located within a CpG island surrounding the TSS and contained 3 restriction sites for the *HpaII* enzyme (CCGG) and 1 restriction site for the *HinPI* enzyme (GCGC). The qPCR product size for this region was 142 bp and the primers sequences were sense: 5'-CTG GTG CTG TTG CTG CAG-3' and antisense: 5'-TGC TCT GGA ACA TCA CCA CC-3'. For the *Agt* gene, the region of interest was a regulatory feature containing a CTCF binding site located 3,000 bp upstream of the TSS. The qPCR product was 125 bp long and contained one restriction site for the *HpaII* enzyme (CCGG). The primers for this qPCR were sense: 5'-CCT GGT GGT CAG ATG CTC TC-3' and antisense: 5'-GGC AGC CTC AGA AAA ACA GC-3'. Amplification and melting curve analyses were performed using the SDS Software version 1.4 (Life Technologies). DNA methylation percentages were calculated as  $\%Me = 100 \times 2^{-(Ct_{Res} - Ct_{NoRes})}$ , where  $Ct_{Res}$  and  $Ct_{NoRes}$  correspond to the  $C_t$  values for the digested DNA and the non-digested DNA aliquot from each sample, respectively. Methylation percentages were normalized against the methylation percentages from SssI-methylated DNA (New England Biolabs).

### Data Analysis

All analyses were conducted using SPSS software (version 21.0; SPSS, Chicago, IL), and data are presented as mean ± SE unless otherwise indicated. Significant differences within groups were analyzed using *t*-tests,  $\chi^2$  tests, nonparametric tests such as the Wilcoxon Signed Rank or Mann-Whitney tests as appropriate, or ANOVA, followed by *post hoc* tests with Bonferroni correction. All *P* values reported are two-tailed with statistical significance set at <0.05.

### ACKNOWLEDGMENTS

A.C. performed experimental procedures, analyzed and interpreted data, and drafted the manuscript. D.G. contributed to study conception and design, analyzed and interpreted data, and finalized the manuscript. R.C. performed experimental procedures, analyzed and interpreted data. Y.W. contributed to study conception and design, performed experimental procedures; analyzed and interpreted data, and finalized the manuscript.

### STATEMENT OF FINANCIAL SUPPORT

This study was supported by Children's Research Foundation grant 2012, Chicago, IL.

Disclosure: None.

### REFERENCES

- Johansson S, Iliadou A, Bergvall N, Tuvemo T, Norman M, Cnattingius S. Risk of high blood pressure among young men increases with the degree of immaturity at birth. *Circulation* 2005;112:3430–6.
- Norman M. Preterm birth—an emerging risk factor for adult hypertension? *Semin Perinatol* 2010;34:183–7.
- Abitbol CL, Rodriguez MM. The long-term renal and cardiovascular consequences of prematurity. *Nat Rev Nephrol* 2012;8:265–74.
- de Jong F, Monuteaux MC, van Elburg RM, Gillman MW, Belfort MB. Systematic review and meta-analysis of preterm birth and later systolic blood pressure. *Hypertension* 2012;59:226–34.
- Dalziel SR, Parag V, Rodgers A, Harding JE. Cardiovascular risk factors at age 30 following pre-term birth. *Int J Epidemiol* 2007;36:907–15.
- Kerkhof GF, Breukhoven PE, Leunissen RW, Willemsen RH, Hokken-Koelega AC. Does preterm birth influence cardiovascular risk in early adulthood? *J Pediatr* 2012;161:390–396.e1.
- Stelloh C, Allen KP, Mattson DL, Lerch-Gaggl A, Reddy S, El-Meanawy A. Prematurity in mice leads to reduction in nephron number, hypertension, and proteinuria. *Transl Res* 2012;159:80–9.
- Nanduri J, Makarenko V, Reddy VD, et al. Epigenetic regulation of hypoxic sensing disrupts cardiorespiratory homeostasis. *Proc Natl Acad Sci USA* 2012;109:2515–20.
- Rogers LK, Velten M. Maternal inflammation, growth retardation, and preterm birth: insights into adult cardiovascular disease. *Life Sci* 2011;89:417–21.
- Wiedmeier JE, Joss-Moore LA, Lane RH, Neu J. Early postnatal nutrition and programming of the preterm neonate. *Nutr Rev* 2011;69:76–82.
- Nuyt AM. Mechanisms underlying developmental programming of elevated blood pressure and vascular dysfunction: evidence from human studies and experimental animal models. *Clin Sci (Lond)* 2008;114:1–17.
- Thompson JA, Regnault TR. In utero origins of adult insulin resistance and vascular dysfunction. *Semin Reprod Med* 2011;29:211–24.
- Gluckman PD, Hanson MA, Cooper C, Thornburg KL. Effect of in utero and early-life conditions on adult health and disease. *N Engl J Med* 2008;359:61–73.
- Giussani DA, Davidge ST. Developmental programming of cardiovascular disease by prenatal hypoxia. *J Dev Orig Health Dis* 2013;4:328–37.
- Barker DJ, Bagby SP, Hanson MA. Mechanisms of disease: in utero programming in the pathogenesis of hypertension. *Nat Clin Pract Nephrol* 2006;2:700–7.
- Pozo ME, Cave A, Koroğlu OA, et al. Effect of postnatal intermittent hypoxia on growth and cardiovascular regulation of rat pups. *Neonatology* 2012;102:107–13.
- Martin RJ, Wang K, Koroğlu O, Di Fiore J, Kc P. Intermittent hypoxic episodes in preterm infants: do they matter? *Neonatology* 2011;100:303–10.
- Farahani R, Kanaan A, Gavrialov O, et al. Differential effects of chronic intermittent and chronic constant hypoxia on postnatal growth and development. *Pediatr Pulmonol* 2008;43:20–8.
- Soukhova-O'Hare GK, Ortines RV, Gu Y, Nozdrachev AD, Prabhu SD, Gozal D. Postnatal intermittent hypoxia and developmental programming of hypertension in spontaneously hypertensive rats: the role of reactive oxygen species and L-Ca2+ channels. *Hypertension* 2008;52:156–62.
- Wang Z, Li AY, Guo QH, et al. Effects of cyclic intermittent hypoxia on ET-1 responsiveness and endothelial dysfunction of pulmonary arteries in rats. *PLoS One* 2013;8:e58078.
- Capone C, Faraco G, Coleman C, et al. Endothelin 1-dependent neurovascular dysfunction in chronic intermittent hypoxia. *Hypertension* 2012;60:106–13.
- Santos MS, Joles JA. Early determinants of cardiovascular disease. *Best Pract Res Clin Endocrinol Metab* 2012;26:581–97.
- Foster GE, Hanly PJ, Ahmed SB, Beaudin AE, Pialoux V, Poulin MJ. Intermittent hypoxia increases arterial blood pressure in humans through a Renin-Angiotensin system-dependent mechanism. *Hypertension* 2010;56:369–77.
- Tamisier R, Pépin JL, Rémy J, et al. 14 nights of intermittent hypoxia elevate daytime blood pressure and sympathetic activity in healthy humans. *Eur Respir J* 2011;37:119–28.
- Julien CA, Kinkead R, Joseph V, Bairam A. Neonatal intermittent hypoxia induces persistent alteration of baroreflex in adult male rats. *Adv Exp Med Biol* 2012;758:179–83.
- Hinderliter AL, Routledge FS, Blumenthal JA, et al. Reproducibility of blood pressure dipping: relation to day-to-day variability in sleep quality. *J Am Soc Hypertens* 2013;7:432–9.
- Hermida RC, Ayala DE, Mojón A, Fernández JR. Blunted sleep-time relative blood pressure decline increases cardiovascular risk independent of blood pressure level—the “normotensive non-dipper” paradox. *Chronobiol Int* 2013;30:87–98.
- Nanduri J, Prabhakar NR. Developmental programming of O(2) sensing by neonatal intermittent hypoxia via epigenetic mechanisms. *Respir Physiol Neurobiol* 2013;185:105–9.
- Reeves SR, Mitchell GS, Gozal D. Early postnatal chronic intermittent hypoxia modifies hypoxic respiratory responses and long-term phrenic facilitation in adult rats. *Am J Physiol Regul Integr Comp Physiol* 2006;290:R1664–71.
- Bassareo PP, Fanos V, Puddu M, et al. Reduced brachial flow-mediated vasodilation in young adult ex extremely low birth weight preterm: a condition predictive of increased cardiovascular risk? *J Matern Fetal Neonatal Med* 2010;23:Suppl 3:121–4.

31. Ligi I, Grandvuillemin I, Andres V, Dignat-George F, Simeoni U. Low birth weight infants and the developmental programming of hypertension: a focus on vascular factors. *Semin Perinatol* 2010;34:188–92.
32. Shechter M, Issachar A, Marai I, et al. Long-term association of brachial artery flow-mediated vasodilation and cardiovascular events in middle-aged subjects with no apparent heart disease. *Int J Cardiol* 2009;134:52–8.
33. Akcakoyun M, Kargin R, Tanalp AC, et al. Predictive value of noninvasively determined endothelial dysfunction for long-term cardiovascular events and restenosis in patients undergoing coronary stent implantation: a prospective study. *Coron Artery Dis* 2008;19:337–43.
34. Schulz E, Gori T, Münzel T. Oxidative stress and endothelial dysfunction in hypertension. *Hypertens Res* 2011;34:665–73.
35. Bogdarina I, Welham S, King PJ, Burns SP, Clark AJ. Epigenetic modification of the renin-angiotensin system in the fetal programming of hypertension. *Circ Res* 2007;100:520–6.
36. Cai J, Tuong CM, Gozal D. A neonatal mouse model of intermittent hypoxia associated with features of apnea in premature infants. *Respir Physiol Neurobiol* 2011;178:210–7.
37. Braga VA, Burmeister MA, Sharma RV, Davisson RL. Cardiovascular responses to peripheral chemoreflex activation and comparison of different methods to evaluate baroreflex gain in conscious mice using telemetry. *Am J Physiol Regul Integr Comp Physiol* 2008;295:R1168–74.
38. Wu HT, Liu CC, Sun CK, et al. Simultaneous assessment of autonomic nervous and vascular endothelial functions in a rat model. *Biomed Tech (Berl)* 2013;58:205–12.
39. Tulppo MP, Mäkikallio TH, Seppänen T, Laukkanen RT, Huikuri HV. Vagal modulation of heart rate during exercise: effects of age and physical fitness. *Am J Physiol* 1998;274(2 Pt 2):H424–9.
40. Peck MA, Crawford RS, Abularrage CJ, et al. A functional murine model of hindlimb demand ischemia. *Ann Vasc Surg* 2010;24:532–7.